

Electronic Switching of Single Silicon Atoms by Molecular Field Effects

Krishnan R. Harikumar, John C. Polanyi,* Peter A. Sloan, Serge Ayissi, and Werner A. Hofer

Contribution from the Department of Chemistry and Institute of Optical Sciences, University of Toronto, 80 St. George Street, Toronto, Ontario, M5S 3H6, Canada and Surface Science Research Centre, The University of Liverpool, Liverpool, L69 3BX, U.K.

Received April 25, 2006; E-mail: jpolanyi@chem.utoronto.ca

Abstract: We have observed on–off switching of scanning tunneling microscope current flow to silicon adatoms of the Si(111)-(7 × 7) surface that are enclosed within a bistable dimeric corral of self-assembled chlorododecane molecules. These thermally activated oscillations amounted to an order of magnitude change in the current. Theory showed that small changes in molecular configuration could cause alterations in the corralled adatom's electronic energy by as much as 1 eV due to local field effects, accounting for the observed current switching.

Introduction

Single-molecule switches have been the subject of numerous experimental and theoretical studies that have tried to understand their behavior and engineer their properties. Molecular conductance has been controlled largely by conformational change in the conducting molecule^{1–3} by external electric fields^{4–6} and subsidiarily by structural changes in the embedding environment.⁷ A recent study demonstrated changes in molecular conductivity due to a local electric field, namely, a single negatively charged silicon dangling bond.⁸ A critical next step is to find a more general means of varying the local electrostatic field. Here, this is accomplished by surrounding a conducting atom by dipolar molecules that switch configuration. The field from the fixed point charge is thus replaced by a variable field. The dipolar molecules consist of a self-assembled halododecane dimer (based on earlier work in this laboratory⁹) that abuts a single silicon adatom on either side. These dimers are shown here to be bistable; they have a high and a low conductance state of the single corralled adatom. A small shift in the dimer's

dipolar end groups changes the induced electric field at the corralled adatom by ~ 1 V, leading to an order of magnitude conductance change of the corralled adatom. This effect is comparable in size to that generated by semiconductor doping. This article demonstrates that small changes in molecular configuration can have substantial effects on the surrounding medium, a finding relevant to molecular electronics and also to biochemistry where links between molecular conformation and function are of importance.¹⁰

Methods

Experiments. We carried out the experiments in ultrahigh vacuum (UHV) using an RHK room-temperature scanning tunneling microscope (STM) or an Omicron variable-temperature STM. All STM bias voltages are sample voltages. Samples were cut from *n*-type (phosphorus-doped) silicon (111) wafers and were resistively flashed in UHV to produce large terraces of Si(111)-(7 × 7). Liquid chlorododecane was repeatedly freeze/pumped/thawed to remove contamination. STM tips were electrochemically etched from 0.38-mm diameter polycrystalline tungsten wire, using a drop-off technique.¹¹

Simulations. Density functional theory simulations on a full unit cell were carried out using the Vienna ab-Initio Simulation Package (VASP).^{12,13} The switching adatom was chosen to be in the faulted half of the unit cell. The molecules were suspended above the silicon 7 × 7 unit cell, and the whole system was fully relaxed until the forces on individual atoms were less than 0.02 eV/Å. The initial position of the chlorine atoms was selected by placing them either above or below the alkane chain in the initial configuration. The Brillouin zone was sampled at the Γ -point only. STM simulations were performed using bSKAN,^{14,15} and the tip model in this case was a tungsten film in (110) orientation with a tungsten pyramid of two layers at the apex.

- (1) Donhauser, Z. J.; Mantooh, B. A.; Kelly, K. F.; Bumm, L. A.; Monnell, J. D.; Stapleton, J. J.; Price, D. W.; Rawlett, A. M.; Allara, D. L.; Tour, J. M.; Weiss, P. S. *Science* **2001**, *292*, 2303.
- (2) Ramachandran, G. K.; Hopson, T. J.; Rawlett, A. M.; Nagahara, L. A.; Primak, A.; Lindsay, S. M. *Science* **2003**, *300*, 1413.
- (3) Moore, A. M.; Dameron, A. A.; Mantooh, B. A.; Smith, R. K.; Fuchs, D. J.; Ciszek, J. W.; Maya, F.; Yao, Y. X.; Tour, J. M.; Weiss, P. S. *J. Am. Chem. Soc.* **2006**, *128*, 1959.
- (4) Blum, A. S.; Kushmerick, J. G.; Long, D. P.; Patterson, C. H.; Yang, J. C.; Henderson, J. C.; Yao, Y. X.; Tour, J. M.; Shashidhar, R.; Ratna, B. R. *Nat. Mater.* **2005**, *4*, 167.
- (5) Chen, J.; Reed, M. A.; Rawlett, A. M.; Tour, J. M. *Science* **1999**, *286*, 1550.
- (6) Reed, M. A.; Zhou, C.; Muller, C. J.; Burgin, T. P.; Tour, J. M. *Science* **1997**, *278*, 252.
- (7) Dameron, A. A.; Ciszek, J. W.; Tour, J. M.; Weiss, P. S. *J. Phys. Chem. B* **2004**, *108*, 16761.
- (8) Piva, P. G.; DiLabio, G. A.; Pitters, J. L.; Zikovskiy, J.; Rezeq, M.; Dogel, S.; Hofer, W. A.; Wolkow, R. A. *Nature* **2005**, *435*, 658.
- (9) Dobrin, S.; Harikumar, K. R.; Jones, R. V.; Li, N.; McNab, I. R.; Polanyi, J. C.; Sloan, P. A.; Waqar, Z.; Yang, J.; Ayissi, S.; Hofer, W. A. *Surf. Sci.* **2006**, *600*, L43.

- (10) Moreno-Herrero, F.; de Jager, M.; Dekker, N. H.; Kanaar, R.; Wyman, C.; Dekker, C. *Nature* **2005**, *437*, 440.
- (11) Guise, O. L.; Ahner, J. W.; Jung, M. C.; Goughnour, P. C.; Yates, J. T. *Nano Lett.* **2002**, *2*, 191.
- (12) Kresse, G.; Hafner, J. *Phys. Rev. B* **1993**, *47*, 558.
- (13) Kresse, G.; Furthmüller, J. *Phys. Rev. B* **1996**, *54*, 11169.
- (14) Hofer, W. A.; Redinger, J. *Surf. Sci.* **2000**, *447*, 51.
- (15) Palotas, K.; Hofer, W. A. *J. Phys.: Condens. Matter* **2005**, *17*, 2705.

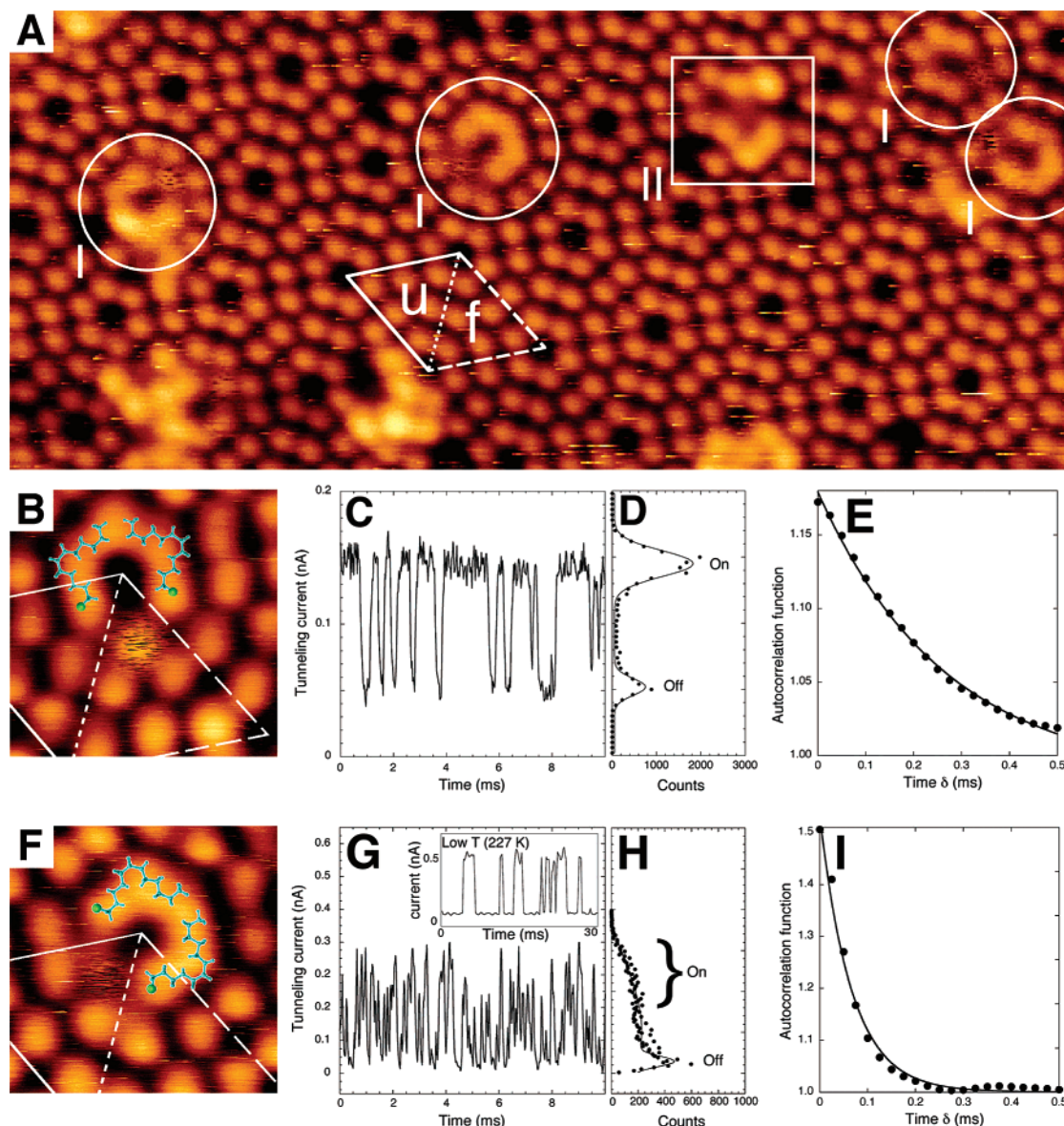


Figure 1. (A) Large-area STM image of a Si(111)-(7 × 7) surface at room temperature after exposure to chlorododecane molecules (230 × 100 Å, +2 V, 0.1 nA). Two types of dimer corral are present: those that surround a corner hole (indicated by circles, labeled type I) and those that surround a corner adatom (indicated by squares, labeled type II). Also marked is a unit cell of the surface indicating the faulted (f) and unfaulted (u) halves. (B and F) High-resolution STM images of a type I corral with the corner adatom that lies in the jaws of the corral belonging to the faulted half of the unit cell (B) and the unfaulted half of the unit cell (F). Each image has two chlorododecane molecules, drawn to scale and superimposed. Chlorine atoms are shown in green, and the alkane chain is blue. (B) 30 × 30 Å, +2.5 V, 0.4 nA; (F) 30 × 30 Å, +2 V, 0.15 nA. (C and G) Tunneling current versus time measurements over (B) a faulted corralled corner adatom at +2.5 V and (F) an unfaulted corralled corner adatom at +2.4 V. (G, inset) Low-temperature (227 K) tunneling current versus time measurements over an unfaulted corralled corner adatom at +2 V. (D and H) The corresponding tunneling current distributions with a pair of Gaussian functions fitted in each case; high-current (on) and low-current (off) states are labeled. (E and I) The auto-correlation of the tunneling current time traces of C and G. The fitted functions are exponential decays (see Methods for details).

Results and Discussion

Figure 1A shows an STM image of a Si(111)-(7 × 7) surface after exposure to chlorododecane at room temperature (see Methods). Pairs of chlorododecane molecules self-assemble through noncovalent bonds into two types of dimer structures, termed type I (around a corner hole) and type II (around a corner adatom). The circles in Figure 1A indicate type I, and the square indicates type II. The type-I structure leaves only one of the six corner adatoms uncovered (Figure 1B,F). This uncovered adatom, located between the jaws of the corral, images as a streaky feature. We shall show that the adatom switches repeatedly between conductance states, leading to its streaky appearance. This adatom, the corralled adatom, is the focus of

this article. Type II corrals form around a central adatom which undergoes charge transfer induced by the corral to create, instead, a stable darkened adatom.⁹

The invariable presence of a streaky corralled adatom only for type I corrals implies that this effect is associated with the corral and is not a tip effect.^{16,17} A chemical change such as C–Cl bond breaking could explain the observed conductance change but the energies of the tunneling electrons (<2.5 eV) are insufficient to break the C–Cl covalent bond of chlorododecane, and we discount this possibility.^{9,18,19} We also rule

- (16) Stroschio, J. A.; Celotta, R. J. *Science* **2004**, *306*, 242.
 (17) Bartels, L.; Meyer, G.; Rieder, K.-H. *Appl. Phys. Lett.* **1997**, *71*, 213.
 (18) Jiang, G. P.; Polanyi, J. C.; Rogers, D. *Surf. Sci.* **2003**, *544*, 147.
 (19) Sloan, P. A.; Palmer, R. E. *Nature* **2005**, *434*, 367.

out extensive changes in the molecular adsorption geometry²⁰ required to bring the halogen atom(s) of the intact alkane halide to within bonding distance of the corralled adatom, as the bright features associated with the adsorbed molecules extend far from the corralled adatom and show little or no change (noise) during imaging. Instead, as we argue below, a more subtle change in the molecular dimer at a distance from the corralled adatom appears to be responsible for the conductance switching.

We have considered the possibility that a mobile impurity hopping between tip and adatom could be the cause of the observed switching, but we have discounted it on the grounds that when switching is halted by cooling there is no detectable (immobilized) impurity, as well as on the further grounds that, as will be shown, alteration in current has no effect on switching rate, and, finally, on the grounds that (in three different UHV machines) switching is invariably present for type I configuration corralls but always absent for type II configuration corralls.

The Si(111)-(7 × 7) unit cell has two electronically distinct halves, faulted and unfaulted (see Figure 1A), that result from the stacking fault layer of silicon atoms. There are therefore two kinds of type I corralled adatom: faulted (Figure 1B) and unfaulted (Figure 1F). We found that these two kinds exhibited different STM imaging properties. A faulted corralled adatom had long streaks, whereas an unfaulted corralled adatom had short streaks. We show below that this results from slow conductance switching and fast conductance switching, respectively. Measurement of the tunneling current into the corralled adatom gives time-resolved information in regard to both the slow and the fast switching.

During an image scan of a type I corral, the raster motion was stopped at preset locations and the feedback loop was disabled. Before resuming the scan, we measured the tunneling current every 25 μs over 0.4 s, building up a time trace of the tunneling current. Figure 1C shows a time trace taken over a faulted corralled adatom, and Figure 1G shows a time trace taken over an unfaulted corralled adatom. The difference in switching rates is apparent. For the faulted corral, the distribution of tunneling currents in the time trace is clearly bimodal (Figure 1D); the corralled adatom was repeatedly switching between two conductance states. We label the high-current state “on” and the low-current state “off”. In the STM images of Figure 1B,F, the on-state corresponds to the corralled adatom’s bright streaks and the off-state corresponds to the dark streaks.

Two pairs of parameters characterize conductance switching: the on-state and off-state tunneling currents, and the on-state and off-state lifetimes. Gaussian functions fitted to the distribution of tunneling currents determined the on-state and off-state tunneling currents, whereas auto-correlation of the time traces determined the lifetimes. The Gaussian fits in Figure 1D for the faulted corral gave an on-state tunneling current of 150 ± 20 pA and an off-state tunneling current of 50 ± 15 pA (errors are the full width at half-maximum). This yields a 3 ± 1 ratio for on-current to off-current for this particular time trace.

A similar analysis for the unfaulted corral (Figure 1H) gave only one fully defined state, the off-state at 30 ± 15 pA. Yet, when cooled, the unfaulted corralls showed two well-resolved states in their time traces (Figure 1G, inset). The unresolved on-state of Figure 1H therefore resulted from the room-

temperature unfaulted corral’s rapid switching being near the limit of our time resolution. To allow these fast switching corralls to be examined, we increased our effective time resolution by analyzing the time traces using the auto-correlation technique, as follows.

Auto-correlation is commonly used to study time-resolved measurements of fluorescence blinking;^{21,22} here we use it to measure the fluctuation in the tunneling current. The maximum correlation occurs at zero delay; at long delay times there is no correlation and the auto-correlation tends to unity. Figure 1E,I shows the auto-correlated time traces of the faulted corral and the unfaulted corral. Both auto-correlation plots displayed an exponential decay. The exponential fits to the auto-correlation yielded the lifetimes of the on-state and the off-state for both the (slow switching) faulted corral and the (fast switching) unfaulted corral (see the Supporting Information for details).

The average on-state lifetime, over a range of tunneling currents, bias voltages, and 11 different type I corralls, was 930 ± 50 μs for the faulted corral. For the off-state lifetime it was 310 ± 20 μs. The faulted corral adatom preferred the on-state. The average on-state lifetime for the unfaulted corral was 150 ± 6 μs, and for the off-state lifetime it was 215 ± 16 μs. The unfaulted corral marginally preferred the off-state. The ratio of on-current to off-current for the faulted corral was 3.8 ± 0.1, which corresponds to a change in the tip height of 0.67 ± 0.01 Å (with the decay constant κ = 1 Å⁻¹). For the unfaulted corral, the tunneling current ratio was 8.7 ± 1.1, corresponding to a tip height change of 1.08 ± 0.06 Å.

We now consider the controlling factors for the conductance switching of the corralled adatom. The exponential decays of the auto-correlations imply that the switching rates (on-to-off and off-to-on) are both stochastic. Two possible sources of excitation that could produce stochastic switching rates are the tunneling current and thermal fluctuations.

A process driven by the tunneling current will have a dependence on the tunneling current and a threshold voltage.^{23,24} Over a range of tunneling currents from 0.1 to 1.2 nA, we found no change for any of the lifetimes. We also found no threshold behavior for the bias dependence of the lifetimes (+2.5 to +0.7 and -0.7 to -2.3 V).²⁵⁻²⁷ Furthermore, within the scatter of the experimental results, the tunneling current ratios were also found to be independent of either tunneling current or bias voltage. It follows that STM-induced electronic effects do not drive the switch.

By contrast, heating the sample above room temperature, as Figure 2A shows, reduced the on-state and off-state lifetimes, while cooling the sample increased their lifetimes. Therefore, thermal fluctuations at constant temperature drive the switch.

-
- (21) Zumbusch, A.; Fleury, L.; Brown, R.; Bernard, J.; Orrit, M. *Phys. Rev. Lett.* **1993**, *70*, 3584.
 (22) Dickson, R. M.; Cubitt, A. B.; Tsien, R. Y.; Moerner, W. E. *Nature* **1997**, *388*, 355.
 (23) Stipe, B. C.; Rezaei, M. A.; Ho, W.; Gao, S.; Persson, M.; Lundqvist, B. I. *Phys. Rev. Lett.* **1997**, *78*, 4410.
 (24) Sloan, P. A.; Hedouin, M. F. G.; Palmer, R. E.; Persson, M. *Phys. Rev. Lett.* **2003**, *91*, 118301.
 (25) At low bias, <±0.5 V, the switch appeared to stop. This we believe to be due to direct tip-surface interaction. At low bias, electrons tunnel into the band gap, and because of the associated low conductivity the tip closely approaches the surface, by ~3 Å from a starting height of ~6 Å, to retain the set point tunneling current.
 (26) Dujardin, G.; Mayne, A.; Robert, O.; Rose, F.; Joachim, C.; Tang, H. *Phys. Rev. Lett.* **1998**, *80*, 3085.
 (27) Shih, C. K.; Feenstra, R. M.; Martensson, P. *J. Vac. Sci. Technol., A* **1990**, *8*, 3379.

(20) Lastapis, M.; Martin, M.; Riedel, D.; Hellner, L.; Comtet, G.; Dujardin, G. *Science* **2005**, *308*, 1000.

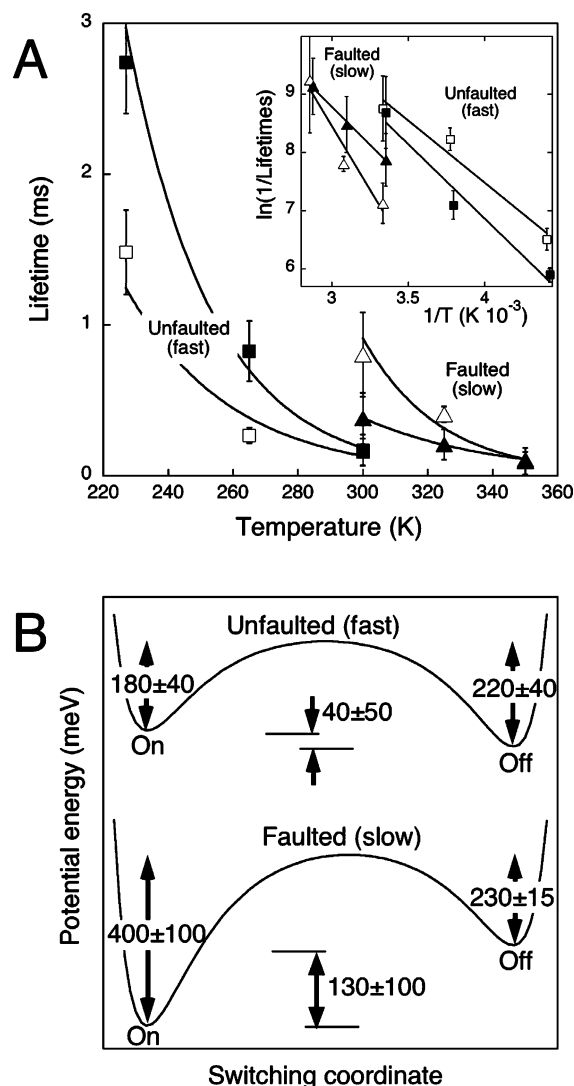


Figure 2. (A) Lifetime as a function of the sample temperature of the faulted on-state (Δ) and off-state (\blacktriangle) and the unfaulted on-state (\square) and off-state (\blacksquare). Fits are exponential. (Inset) Arrhenius plot with linear fits. (B) Schematic of the potential energy, derived from the Arrhenius fits, for the faulted and unfaulted corralled adatoms.

By fitting the Arrhenius equation to the temperature dependence of the lifetimes (Figure 2A, inset), we calculated the activation energies and pre-exponential A-factors for the switching processes. Figure 2B presents the activation energies as two schematic potential energy curves. The average pre-exponential A-factor was $10^{7.5 \pm 0.5} \text{ s}^{-1}$, much lower than the standard value of 10^{13} s^{-1} .^{28,29} Reduced A-factors have been associated with thermally induced charge transfer from the substrate to adsorbate.³⁰ To determine if such processes are involved in the switching, further experiments with different surface doping would be required; these lie outside the scope of the present study.

To probe the molecular properties that govern the conductance switching, we formed type I corrals from different halogenated alkanes. Changing the length of the alkane chain from 12 carbon atoms (chlorododecane) to 10 carbon atoms (chlorodecane) did

not measurably affect the on-state and off-state lifetimes.³¹ Similarly, changing the halogen atom from Cl to F did not significantly change the on-state lifetime: $200 \pm 60 \mu\text{s}$ for a fluorododecane corral and $150 \pm 6 \mu\text{s}$ for a chlorododecane corral. However, this change of halogen, Cl to F, increased by more than a factor of three the off-state lifetime: $710 \pm 130 \mu\text{s}$ for a fluorododecane corral as compared to $215 \pm 16 \mu\text{s}$ for a chlorododecane corral. It appears that the conductance switching of the corralled adatom is controlled by atoms toward the halogen end of the corralling molecules.

The surface itself, faulted and unfaulted, also affected the conductance switching. As already noted, the two halves of the Si(111)-(7 × 7) unit cell gave different switching rates. To explore this surface effect, we combined our time-resolved measurements with the spatial resolution of the STM to form a map of the ratio of on-state to off-state tunneling currents, that is, the switching amplitude. These maps are presented in Figure 3A for a faulted corral and Figure 3B for an unfaulted corral. The faulted map contains data from 234 time traces taken over 35 different faulted corrals. Similarly, the unfaulted map contains data from 348 time traces taken over 47 different unfaulted corrals. The symmetry of the corral/substrate system imposes a vertical mirror plane in the switching maps.³² Most striking is the location of the switch; for the unfaulted corral (Figure 3B) the switch is centrally located between the corralled adatom and its neighboring rest atom; the faulted corral (Figure 3A) also has a large switching ratio at the equivalent location but is more dispersed, extending into the location of the corralled adatom. This result mirrors the location of the switching effect observed in high-resolution STM imaging (Figure 3C,D).

The difference between faulted and unfaulted regions is the location of the subsurface silicon atom in the stacking fault layer. For the faulted section, the stacking fault atom is directly below the corralled adatom, whereas for the unfaulted section it is halfway between the corralled adatom and the neighboring rest atom. Therefore, there appears to be some correlation between the location of the stacking fault atom and the location of the switch. We tentatively propose that the stabilization energy of the on-state is dependent on the stacking fault atom, so that when this atom is close to the corral (faulted) the on-state potential is twice as deep than when it is further away (unfaulted); $\sim 400 \text{ meV}$ rather than $\sim 200 \text{ meV}$.

To determine whether configuration changes could account for the conductance switching of the corralled adatom, we performed density functional calculations and electron transport (STM) simulations on a chlorododecane corral with a faulted corralled adatom (see Methods). In the calculations, we indeed found two stable adsorption configurations that are shown in Figure 4A. We show below that these configurations correspond to an on-state (blue molecules of Figure 4A) and an off-state

(31) A faulted chlorododecane corral (10 carbons) had an on-state lifetime of $800 \pm 40 \mu\text{s}$ and an off-state lifetime of $380 \pm 60 \mu\text{s}$, which are similar to the chlorododecane (12 carbons) on-state lifetime of $930 \pm 50 \mu\text{s}$ and off-state lifetime of $310 \pm 20 \mu\text{s}$. The unfaulted chlorododecane (10 carbons) corral had an on-state lifetime of $160 \pm 20 \mu\text{s}$ and an off-state lifetime of $170 \pm 25 \mu\text{s}$, again similar to the chlorododecane (12 carbons) on-state lifetime of $150 \pm 6 \mu\text{s}$ and off-state lifetime of $215 \pm 16 \mu\text{s}$.

(32) Because of their negligible switching amplitude, time traces taken far removed from the center of the switching effect often lead to numerical instabilities in the auto-correlation analysis. We imposed the following acceptance criteria to remove unreliable data from the switching maps of Figure 3A,B: for the faulted corral only time traces with an "on" lifetime less than 1400 ms and an "off" lifetime greater than 330 ms were included, and for the unfaulted corral only time traces with an "on" lifetime less than 330 ms and an "off" lifetime less than 550 ms were included.

(28) Mayne, A. J.; Lastapis, M.; Baffou, G.; Soukiasian, L.; Comtet, G.; Hellner, L.; Dujardin, G. *Phys. Rev. B* **2004**, *69*, 045409.

(29) Lauhon, L. J.; Ho, W. *J. Chem. Phys.* **1999**, *111*, 5633.

(30) Trenhaile, B. R.; Antonov, V. N.; Xu, G. J.; Nakayama, K. S.; Weaver, J. H. *Surf. Sci.* **2005**, *583*, L135.

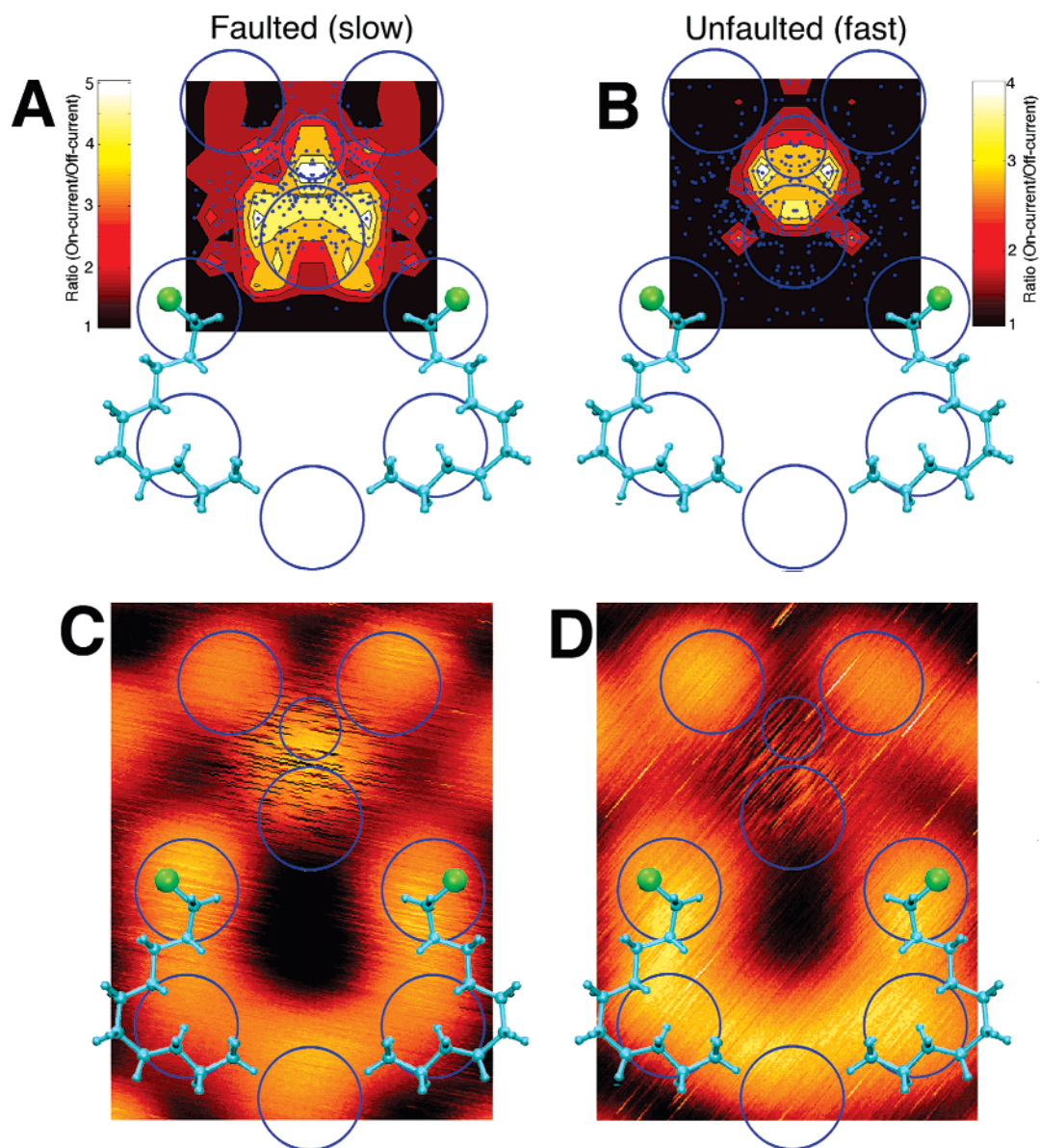


Figure 3. (A and B) Plan view spatial maps of the ratio of on-state tunneling current to off-state tunneling current for chlorodecane type I corrals with (A) a faulted corralled adatom and (B) an unfaulted corralled adatom (see side bar for color code). Large blue circles represent silicon adatoms, and the smaller blue circle represents a rest atom. Blue dots indicate the position of individual time-trace measurements. A vertical plane of symmetry exists in the dimer/surface system, and this symmetry was imposed in the switching maps. (C and D) STM images of Figure 1B,F shown with adatoms and rest atoms indicated to allow easy comparison.

(red molecules of Figure 4A) of the corral. Given the size of the molecules, we cannot be certain that these configurations are unique. In accord with the interpretation of the experiments given above, the main geometric difference between the pair of configurations is the position of the chlorine end of the molecule; the terminal chlorine ends of the molecules are either closer (off-state) or further away (on-state) from the corralled adatom.

The calculated energy difference between the two configurations was 270 meV. However, it should be noted that owing to the large size of the simulated unit cell the precision of the calculation, which is satisfactorily small at 1 meV per atom, amounted to a total energy uncertainty of ~ 300 meV. For this reason, we consider the energies of the two configurations equal within the limits of the calculation. Nonetheless, the simulations establish that the molecular arrangements have a small enough energy difference that they can be altered in a thermally driven

process. In this process, the chlorine ends of the molecules alternate their distance from the corralled adatom. In neither configuration, however, is the chlorine nearer than 6 to 7 Å from the corralled adatom; too far it would appear for even weak chemical bonding.

While the computed configuration changes from the on-state to the off-state appear to be minor, they have a substantial effect on the electron states at the position of the corralled adatom. Figure 4B,C reveals that the height of the calculated charge density contour at the corralled (top) adatom changes by more than 0.5 Å. Successive contour lines in these plots describe a height variation of 0.5 Å.

To compute the changes in the tunneling current flowing into the corralled adatom, we performed STM simulations with a (theoretical) tungsten tip. Figure 4D,E presents the simulated STM images of the two molecular geometries shown in Figure 4A. It can be seen that depending on the configuration of the

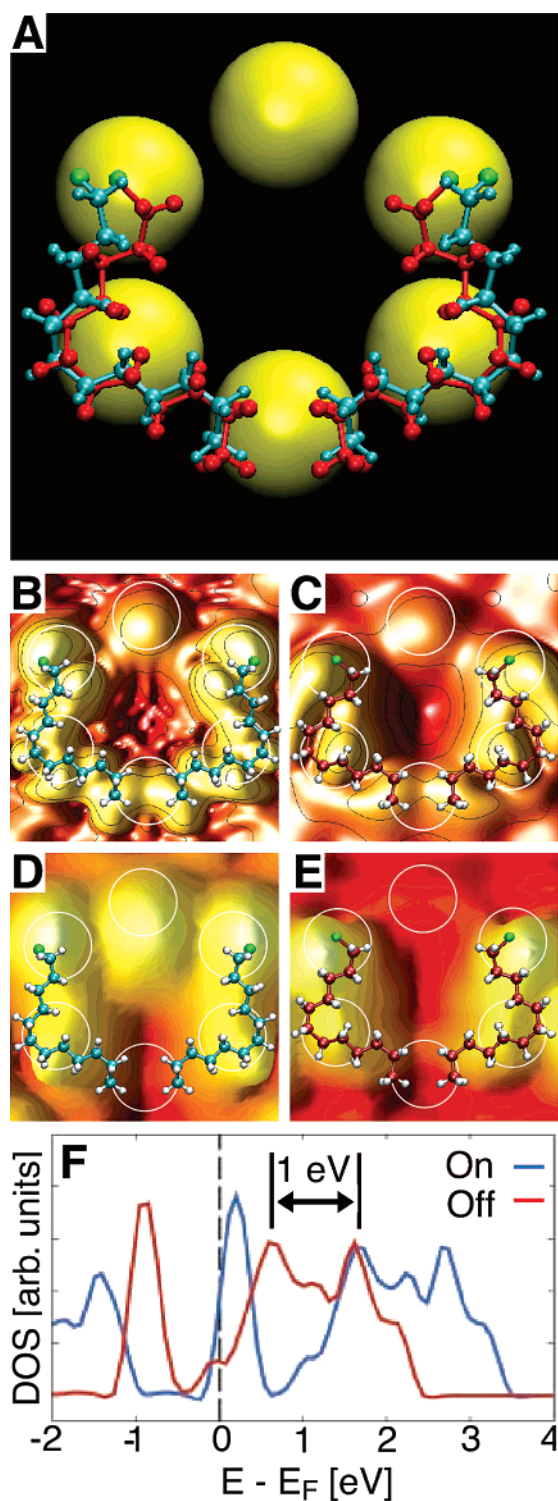


Figure 4. Density functional theory and transport simulations of the switch. (A) Molecular configurations: on-state (blue molecules) and off-state (red molecules). (B and C) Density contours from E_F to $E_F + 2$ eV, value 10^{-5} e/Å³. The contour lines correspond to a vertical distance of 0.5 Å. White circles indicate the silicon adatoms at the corner hole. (D and E) Simulated STM constant current contours (+2 V, 50 pA). (D) On-state. (E) Off-state. The difference in apparent height measured at the top of the adatom is 1 Å. (F) DOS integrated over the silicon adatom. The DOS is bodily shifted by 1 eV, indicating the change of the dipole field due to molecular configurations.

molecules the corralled adatom appears either as a distinct protrusion (Figure 4D) or as a “missing” feature (Figure 4E). The computed height difference between the two states of the

corralled adatoms is 1 Å, comparable to the experimental height difference of ~ 0.7 Å. These two states of the molecules thus correspond to the on-state and off-state of the corral. The switching behavior is established as being dependent on small changes in the position of the polar end of the molecules.

We note the absence of tunneling current in the theoretical STM images of Figure 4D,E to the adatom at the bottom of the corral. This is despite the fact that Figure 4B,C shows a high DOS at this location. We attribute this to a numerical artifact stemming from the finite size of the simulated STM tip.³³

We found previously that the molecular chlorododecane type II corrals induce static lateral surface dipoles in the silicon surface, which are accompanied by substantial charge transfer along the surface.⁹ The occurrence of the surface dipoles was related to the formation of a corral. Here, we find that the type I induced surface dipoles are switched on and off by the configuration of the molecules. This can be seen in the analysis of the density of states (DOS) at the position of the corralled adatom. Figure 4F shows that the off-state of the molecules corresponds to a bodily downward shift of the DOS, relative to the on-state, at the corralled adatom by about 1 eV. The DOS also reveals that the main contribution to the tunneling current originates from the lowest unoccupied state at the position of the adatom (see the distinct peak at low positive energy). This state is shifted below the Fermi level in the “off” configuration, which means that in this case it carries additional electron charge. A similar shift to lower energies has been observed in our previous work.⁹

This type of DOS shift is only observed if an electrostatic field is applied to the surface at this location. From the simulated STM images and the corresponding changes in configuration, we therefore conclude that the small configuration changes induce electric fields in the vicinity of the corral, which amount to an electrostatic potential of about 1 V. Given that defect atoms in semiconductors (e.g., dopants³⁴) show effects of a similar magnitude, we conclude that modest molecular configuration changes can produce effects equal in magnitude to the effects of chemically doping a semiconductor. However, the effect in this case is not due to localized charges, but due to a substantially enlarged dipole field in the “off” configuration. We find that the lateral dipole moment in the off-state is increased by a factor of 7. Due to the decay characteristics of dipole fields, proportional to the inverse square of the distance, the effect is limited to a very small region of the surface, in contrast to charges at dangling bonds,⁸ where the Coulombic field decays with the inverse distance.

In summary, we report a single-atom electronic switch in silicon due to molecularly induced field effects. Small changes in configuration of a self-assembled pair of dipolar adsorbate molecules that surround a silicon atom are shown to have a large electronic effect characterized by a high and a low

(33) A real STM tip is semi-infinite, which renders the energy distribution relatively flat over the whole bias regime. By contrast, STM tip models consist of a finite number of metal layers due to numerical limitations. This introduces quantum confinement into electronic states and a variation of the density of states with energy. If, as in the case of carbon–carbon and carbon–hydrogen bonds, the available states at the molecule are highly discrete, this may introduce a mismatch of eigenvalues of tip and surface electronic states, which leads to a reduced current flow at discrete energy values. In this case, a part of the molecule may appear darker than in the experiments.

(34) On GaAs, the substitution of a Ga atom by Si, for example, shows an equivalent shift of the eigenstates by 1 eV. Pereira-Borrajó, N.; Hofer, W. A.; Lundgren, E. Unpublished results; Surface Science Research Centre, The University of Liverpool (2006).

conductance. The finding that small changes in conformation of molecules can have substantial external electronic effects should be of interest in contexts ranging from nanoscale electronics to molecular biology.

Acknowledgment. We are indebted to the Natural Science and Engineering Research Council of Canada (NSERC); Photonics Research Ontario (PRO), an Ontario Centre of Excellence; the Canadian Institute for Photonic Innovation (CIPI); and the Canadian Institute for Advanced Research (CIAR) for their support of this work. P.A.S. thanks the Royal Society for an

International Research Fellowship. S.A. is funded by EPSRC Grant GR/T20366/01. W.A.H. is supported by a University Research Fellowship of the Royal Society. We thank Kurt W. Kolasinski and Kalle Ernst for helpful discussions.

Supporting Information Available: Auto-correlation. This material is available free of charge via the Internet at <http://pubs.acs.org>.

JA062874C